Available online at www.sciencedirect.com

ScienceDirect

Underground Space 16 (2024) 301–313

www.keaipublishing.com/undsp

Research Paper

Performance comparison of machine learning algorithms for maximum displacement prediction in soldier pile wall excavation

Danial Sheini Dashtgoli [a,b,*], Mohammad Hossein Dehnad [c], Seyed Ahmad Mobinipour [c], Michela Giustiniani [b]

[a] Department of Mathematics, Informatics, and Geosciences, University of Trieste, Trieste 34127, Italy
[b] National Institute of Oceanography and Applied Geophysics-OGS, Borgo Grotta Gigante 42/C, Trieste, Sgonico 34010, Italy
[c] Department of Civil Engineering, University of Qom, Qom 3716146611, Iran

Received 28 February 2023; received in revised form 3 August 2023; accepted 9 September 2023
Available online 9 January 2024

Abstract

One of the common excavation methods in the construction of urban infrastructures as well as water and wastewater facilities is the excavation through soldier pile walls. The maximum lateral displacement of pile wall is one of the important variables in controlling the stability of the excavation and its adjacent structures. Nowadays, the application of machine learning methods is widely used in engineering sciences due to its low cost and high speed of calculation. This paper utilized three intelligent machine learning algorithms based on the excavation method through soldier pile walls, namely eXtreme gradient boosting (XGBoost), least square support vector regressor (LS-SVR), and random forest (RF), to predict maximum lateral displacement of pile walls. The results showed that the implemented XGBoost model performed excellently and could make predictions for maximum lateral displacement of pile walls with the mean absolute error of 0.1669, the highest coefficient of determination 0.9991, and the lowest root mean square error 0.3544. Although the LS-SVR, and RF models were less accurate than the XGBoost model, they provided good prediction results of maximum lateral displacement of pile walls for numerical outcomes. Furthermore, a sensitivity analysis was performed to determine the most effective parameters in the XGBoost model. This analysis showed that soil elastic modulus and excavation height had a strong influence on of maximum lateral displacement of pile wall prediction.

Keywords: Soldier pile wall; Lateral displacements; XGBoost; Machine learning; Artificial intelligence

1 Introduction

Deep excavation is now required today for a variety of projects, including the construction of underground facilities, water and sewage pumping stations, underground stations, and the high-rise building basements. Especially in urban construction, the safety and serviceability of surrounding structures are at risk if the displacement of the excavation exceeds a certain level. As a result, determining the maximum displacement of a deep excavation is a crucial global problem. Engineers and researchers have conducted a detailed analysis of lateral wall displacement due to excavation. To date several research papers have investigated the behaviour of different walls affected by deep excavations, including diaphragm walls (Addenbrooke et al., 2000; Bica & Clayton, 1998; Dong et al., 2014; Elbaz et al., 2018; Goh et al., 2017; Hashash & Whittle, 1996; Hsiung, 2009; Hsiung et al., 2016; Kunasegaram & Takemura, 2021; Ou et al., 2020; Tan & Wei, 2012), sheet piling (Gajan, 2011; Gopal Madabhushi & Chandrasekaran, 2005; Wong & Broms, 1989), nailing (Cheuk et al., 2005; Hu et al., 2020; Liu et al., 2021;

* Corresponding author at: Department of Mathematics, Informatics, and Geosciences, University of Trieste, Trieste 34127, Italy.
E-mail address: dsheinidashtgoli@ogs.it (D. Sheini Dashtgoli).
Peer review under the responsibility of Tongji University.

https://doi.org/10.1016/j.undsp.2023.09.013
2467-9674/© 2024 Tongji University. Publishing services by Elsevier B.V. on behalf of KeAi Communications Co. Ltd.
This is an open access article under the CC BY-NC-ND license (http://creativecommons.org/licenses/by-nc-nd/4.0/).

Singh & Sivakumar Babu, 2010; Yuan et al., 2019), and soldier pile wall (Vermeer et al., 2001; Athmarajah & de Silva, 2019; Chalmovsky et al., 2011; Hong et al., 2003; Lee et al., 2011; Perko & Boulden, 2008; Rashidi & Shahir, 2019; Ye & He, 2022; Zhang et al., 2022). Ramadan et al. (2018) conducted a parametric study to evaluate three factors, namely excavation depth, wall stiffness, and pile embedment depth for shallow excavation in clay medium using the three-dimensional finite element method. Various design proposals for a safe support system were then made. In order to establish a trustworthy representation of the functioning of slip-resistant pile structures, Buslov and Margolin (2018) conducted an analytical study on the subject of retaining walls with multiple rows of piles and evaluated the function of the second row during their operation. Ramadan and Meguid (2020) provided the results of a single numerical analysis to determine the activities of a cantilever secant pile wall used to support an excavation in sand. This parametric study used a wide range of sand density, excavation depth, flexural stiffness of wall, and bonding between piles within the wall. Based on the results, a model was developed to predict the deflection of the wall in the presence of fully and partially bonded piles. Bekdaş et al. (2020) investigated cantilever soldier pile retaining walls embedded in friction soils in order to balance cost and size while meeting geotechnical and structural criteria. Razeghi et al. (2021) performed nine centrifuge experiments to investigate the effects of different geometric elements, such as pile spacing ratio and pile embedded depth ratio, on wall lateral displacement, pile bending moment, and backfill settlement. The centrifuge data suggested that reducing pile area and increasing the pile embedment depth would reduce the settlement of cantilever pile walls.

The three main methods used to predict the deformation of concrete walls caused by excavation are analytical and semi-analytical solutions, numerical simulations, and experimental studies. However, the predicted results are usually exaggerated. The empirical formulas based on previous work have a very simple model and are not particularly sophisticated in application. Although numerical simulation techniques like the finite element and finite difference methods often provide more accurate results, they are challenging due to the complexity of bringing together all instinctive and extinct components. In addition, experimental methods lead to very costly projects and require advanced instrumentation.

Nowadays, the use of engineering problem-solving methods using artificial intelligence algorithms is very beneficial in various fields such as medicine, environment and oil industry, construction, and all other sciences with the development of computer science and advanced machine learning algorithms and access to valuable data. Machine learning (ML), a relatively new technology in the field of geotechnical engineering, has attracted great interest due to its high efficiency, superior generalisation performance, and ability to handle problems in large-scale. Also, ML methods have proven useful in predicting geomechanical parameters, such as the tensile strength of rock materials (Ceryan et al., 2013), assessing seismic-liquefaction potential (Samui et al., 2011), and predicting slope stability conditions (Samui, 2013). These techniques have been applied in different fields, such as the behavior of structural elements like diaphragm walls, sheet pile walls, and braced walls, as well as in analysing the performance of piles and evaluating ground surface settlement due to excavation activities (Alkroosh & Nikraz, 2012; Ismail & Jeng, 2011; Samui, 2011; Su et al., 2022). In addition, several researchers have studied various properties of diaphragm walls. Jan et al. (2002) selected 18 case studies of deep excavations with four to seven excavation phases to train and test the prediction of diaphragm wall displacement by a supervised neural network. A study on deep excavations, mostly in soft soils, was conducted by Moormann (2004) using a comprehensive database of over 530 recent worldwide case studies. Kung et al. (2007) used an artificial neural network (ANN) approach to predict deflection that would occur in supported excavation in soft to medium clay. The convolutional neural network (CNN) model was found to be the most suitable model for predicting diaphragm wall deflection and was able to provide adequate guidance for site safety management. Zhang et al. (2020) compared the prediction performance of soft computing techniques such as XGBoost, multivariate adaptive regression splines (MARS), ANN, and support vector machine (SVM) in a case study for estimating maximum lateral wall deflection in supported excavation. Using three ML algorithms, namely back-propagation neural network, long short-term memory (LSTM), and gated recurrent unit (GRU), Zhao et al. (2021) predicted the concrete diaphragm wall caused by excavation. They showed that GRU outperformed LSTM in terms of computational time, which exhibited lower prediction errors, and demonstrated greater robustness in a 10-fold cross-validation. Later, the effects of soft clay anisotropy on diaphragm wall deformations in a braced excavation were determined based on the results of finite element analysis (Zhang et al., 2021). Huang et al. (2022) proposed an ANN approach to predict the horizontal displacement of tunnels in soft soils caused by excavation. ANN model was developed using a series of finite element data sets obtained from verified numerical models. Seven input variables were selected, including excavation width and depth, retaining wall thickness, average shear strength, average modulus of elasticity for unloading and reloading, horizontal distance between the tunnel and retaining wall, and burial depth of tunnel crown. The feasibility of the developed ANN model to predict the horizontal displacement of the tunnel due to excavation was demonstrated by the results obtained.

Recently, ANN was used by Pradeep et al. (2022) to predict the embedment depth of a cantilever sheet pile wall in the context of sheet piling. Soil properties such as cohesive-

ness, internal friction angel, and unit weight were employed as input factors to determine the expected embedment depth of the pile. Akan (2022) demonstrated how expressions derived using multiple linear regression (MLR) analysis can be used to determine where the maximum bending moment (M_{max}) would occur in the cross-section of a cantilever sheet pile wall penetrating sand. The results showed that polynomial equations can be used in addition to MLR models to achieve M_{max}. Afterward, fully braced excavations in inhomogeneous soils were examined for stability using a two-dimensional plane strain-based finite element limit analysis approach (Yodsomjai et al., 2022). However, to generate the equation for stability prediction, the model MARS was used, which is a machine regression method commonly used by experts in the field. Zhang et al. (2022) proposed a method based on automatic ML to address the problem precisely so that they could determine the effects of a deep excavation on nearby existing shield tunnels. Their model was acceptable for the application in real construction projects, as shown by the agreement of the prediction results with the monitoring data. Huang et al. (2021) proposed a method for calculating the expected deflection of a cantilever wall in undrained clay using an ANN-based tool. Their results showed that the proposed model could reliably predict the deflection of a cantilever wall in undrained clay. The sensitivity analysis also revealed that the excavation depth had the greatest influence. The state of deep learning (DL) practice in geotechnical engineering was provided by Zhang et al. (2021), who also showed the statistical trend of published papers. In terms of geotechnical applications, four main algorithms were developed: feedforward neural network, recurrent neural network, CNN, and generative adversarial network. Furthermore, the challenges and perspectives for DL development in geotechnical engineering were mentioned and discussed.

2 Research aims and objectives

Based on the present literature review, there is a significant lack of using ML algorithms for rapid prediction of maximum lateral displacement of deep excavations constructed with soldier pile walls. Therefore, this study proposes three intelligent ML methods for predicting maximum lateral displacement of deep excavations constructed by soldier pile walls. This research can be divided as follows. Firstly, we introduce the idea of ML and several complementary modeling techniques. Secondly, we describe the databases and pre-processing techniques we use to prepare the data for analysis. We then analyse the applicability and generality of the three algorithms XGBoost, LS-SVR and RF together with the ML and compare the derived results to show the excellent fit and predictive ability of the model.. A ranking of the influence of deep excavation factors on lateral displacement is done as the final step of the analytical process. The results are then summarised.

3 Methodology

3.1 Workflow

The input parameters for training ML models are two excavation dimensions (called B and L), excavation height (H), soil elasticity (E_s), pile height (H_p), soil friction angle (φ), soil cohesion (C), soil unit weight (γ), pile diameter (D_p), wale width (W_w), pile spacing (S_p), and shotcrete thickness (t). Figure 1 shows the major steps of proposed methodology. The details of the individual processes are explained in the following section.

3.2 Database introduction

3.2.1 FEM model

Although deep excavations with soldier pile walls are carried out in a number of engineering scenarios, data collection in the field is quite tedious. Important parameters are often missing from existing data, and there is insufficient mass to produce an estimate. This problem was solved by creating a database for numerical modelling of the maximum lateral displacement of soldier pile walls. Figure 2 shows the typical geometry used for numerical modelling. First, the finite element model (FEM) is verified using data from a high-quality excavation project with extensive documentation (Chavda et al., 2019); A database was then created by building 675 different models based on variable features. The reliable database is then used to develop ML estimators.

The mathematical statistics on the database variables are calculated and presented in Table 1 to provide better understanding of data distribution. The extreme values of the variables are labeled Max and Min. The mean value represents the average, while standard deviation (SD) represents the degree of dispersion. The twelve database components previously examined in the context of deep excavation serve as input variables for this study. The maximum displacement of pile wall is treated as target in the ML models, and it is present in the database as the output (U).

3.2.2 Database processing

Before using the data to build ML models from the original database, a number of data processing techniques should be performed to improve the quality of the data. First, the training set is randomly selected from the 675 records in the database, and the test dataset is created from the remaining 30%, 25%, and 20%. The ideal ratio for splitting up the data is determined and set during evaluation process. The 3-, 5-, 10-, and 15-fold cross-validation procedure is then used to create the validation set for the model training process. This improves the robustness of the model. Along with the above pre-processing techniques, the Optuna package (Akiba et al., 2019) is used to find the best set of hyperparameters. The training dataset is used to train ML models, which are then tested on an inde-

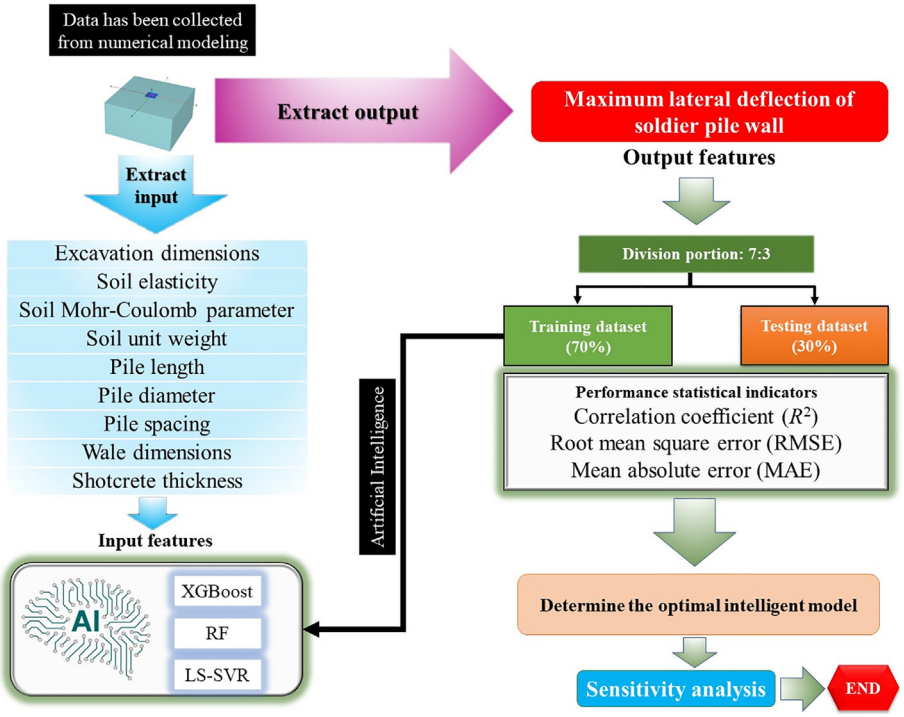

Fig. 1. Workflow adopted in this study.

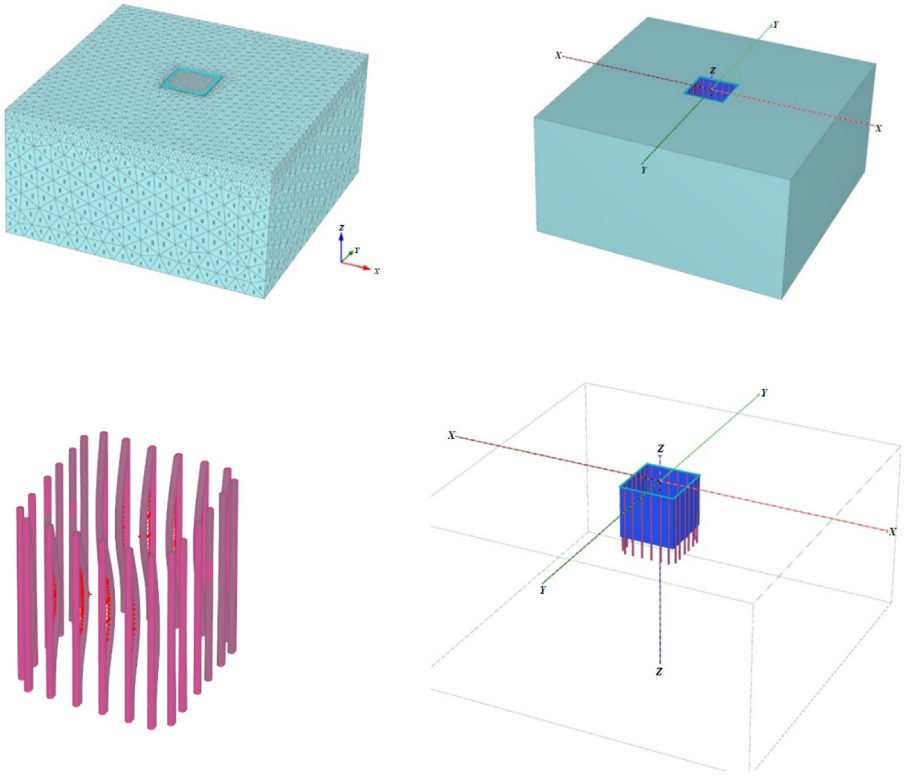

Fig. 2. Three-dimensional FEM concept.

pendent dataset (the test dataset). The ML models are built according to the schema in Fig. 1.

Scatter plots are appropriate 2D plots for showing the relationship between two variables in a dataset. The *X*-axis represents an independent variable or attribute, while the *Y*-axis represents a dependent variable. Figure 3 shows the relationship between 12 features and the maximum deflection of the soldier pile wall. Accordingly, the

Table 1
Statistical description of database created.

Feature	B (m)	L (m)	H (m)	H_p (m)	D_p (m)	S_p (m)	t (mm)	γ (kN/m^2)	E_s (MPa)	C (kPa)	φ (°)	W_w (m)	U (mm)
Mean	9.69	13.69	11.92	16.07	1.00	1.95	9.69	19.58	28.35	15.92	29.14	1.24	15.30
SD	3.57	3.10	4.18	5.40	0.11	0.54	1.38	0.79	15.00	5.39	4.09	0.06	12.20
Min	4.00	8.00	5.00	7.00	0.85	1.00	8.00	18.70	15.00	10.00	25.00	1.10	0.02
Max	16.00	17.00	15.00	20.00	1.20	3.00	12.00	21.00	55.00	25.00	36.00	1.30	49.02

increases in excavation height, pile height, and pile spacing lead to a significant increase in maximum displacement and the decreases in cohesion, soil friction angle, soil elastic modulus, pile diameter, and soil unit weight, resulting in a significant decrease in the output target.

Figure 4 shows the correlation heat map of the features derived from the database. A correlation heatmap is a visual representation of a correlation matrix showing the degree of correlation between different variables. Heat maps are a two-dimensional representation of data, where values are colour-coded to indicate their respective intensities. A heat map can be used to summarise data quickly and easily. In addition, complex datasets can be better understood with the help of more detailed heatmaps. A straight line can be drawn from top left to bottom right to show how well each variable correlates with itself. This is a symmetrical matrix as the correlations above and below the primary diagonal are mirror images of each other. As it can be seen, the correlation between U and H, H_p, E_s, as well as B and L are very strong with the coefficients of 0.71, 0.71, −0.51, 0.54, and 0.62, respectively.

4 Modelling theory

4.1 XGBoost

The scalable end-to-end tree boosting system XGBoost is widely used in data science. This technology gives data scientists access to state-of-the-art solutions to a range of ML problems. It is relevant for both classification and regression problems. Due to its high execution speed and efficient out-of-core processing, XGBoost is the algorithm of choice among ML researchers. The gradient boosting approach combines weak classifiers or regressors into a single robust predictive model. The final model is built using a method that iteratively adds weak students one by one to an ensemble. To prevent overfitting, XGBoost algorithm has improved a basic gradient boosting technique by incorporating a regularisation component Eq. (2) into the objective function Eq. (1) (Chen & Guestrin, 2016).

$$\text{Obj} = \sum_{i=1}^{n} l(y_i, \hat{y}_i) + \sum_{k=1}^{K} \Omega(f_k), \tag{1}$$

where $\hat{y}_i$ is the prediction at the i-th round; y_i is the real value; $l(y_i, \hat{y}_i)$ is the loss function; f_k is the term used to describe the decision tree structure; $\Omega(f_k)$ is the regularization term; n is the number of training examples.

$$\Omega(f_k) = \gamma T + \frac{1}{2}\lambda\|\omega^2\|, \tag{2}$$

where γ is used to regulate the number of leaf nodes; T is the number of leaves; λ is to keep the leaf node score within acceptable limits to avoid overfitting; ω is the leaf node's score.

Each feature point is repeatedly evaluated by XGBoost based on its value in the above objective function using a greedy method. The objective function gain of a single leaf node is compared exactly with the value of the split objective function within a predefined threshold that severely restricts the development of tree, and the split is only performed if the gain exceeds the threshold. Therefore, it is important to describe the top characteristics and branch points that will ultimately establish the tree structure. Working with XGBoost requires careful parameter tuning and can lead to overfitting for small or noisy data sets. It can also become computationally intensive when working with large data sets.

4.2 Least squares support vector machine model

The Least Squares Support Vector Machine model (LS-SVM) is a variant of the SVM developed for function estimation or regression tasks proposed by Suykens et al. (2002). It combines the principles of SVM with the concept of least squares regression to create a powerful model for accurate approximation of functions. In LS-SVM, the objective is to find a hyperplane that effectively fits the training data and accurately predicts the target variable for new unseen data points. This is achieved by minimising the squared norm of the weight vector, where the predicted outputs obtained by applying the weight vector and the bias term to the feature representation of the input data should be within a certain tolerance of the actual targets. The optimization of LS-SVM is to find the optimal values for the weight vector and the bias term. To achieve this, linear equations or optimization techniques such as quadratic programming can be utilized. In addition, the model includes parameters such as the regularisation parameter, which controls the trade-off between fitting the training data and avoiding overfitting, and the kernel function parameters, which define the mapping of the input data into a higher-dimensional feature space. Once the LS-SVM model is trained and optimized, it can be used to estimate target values for new input data by using the

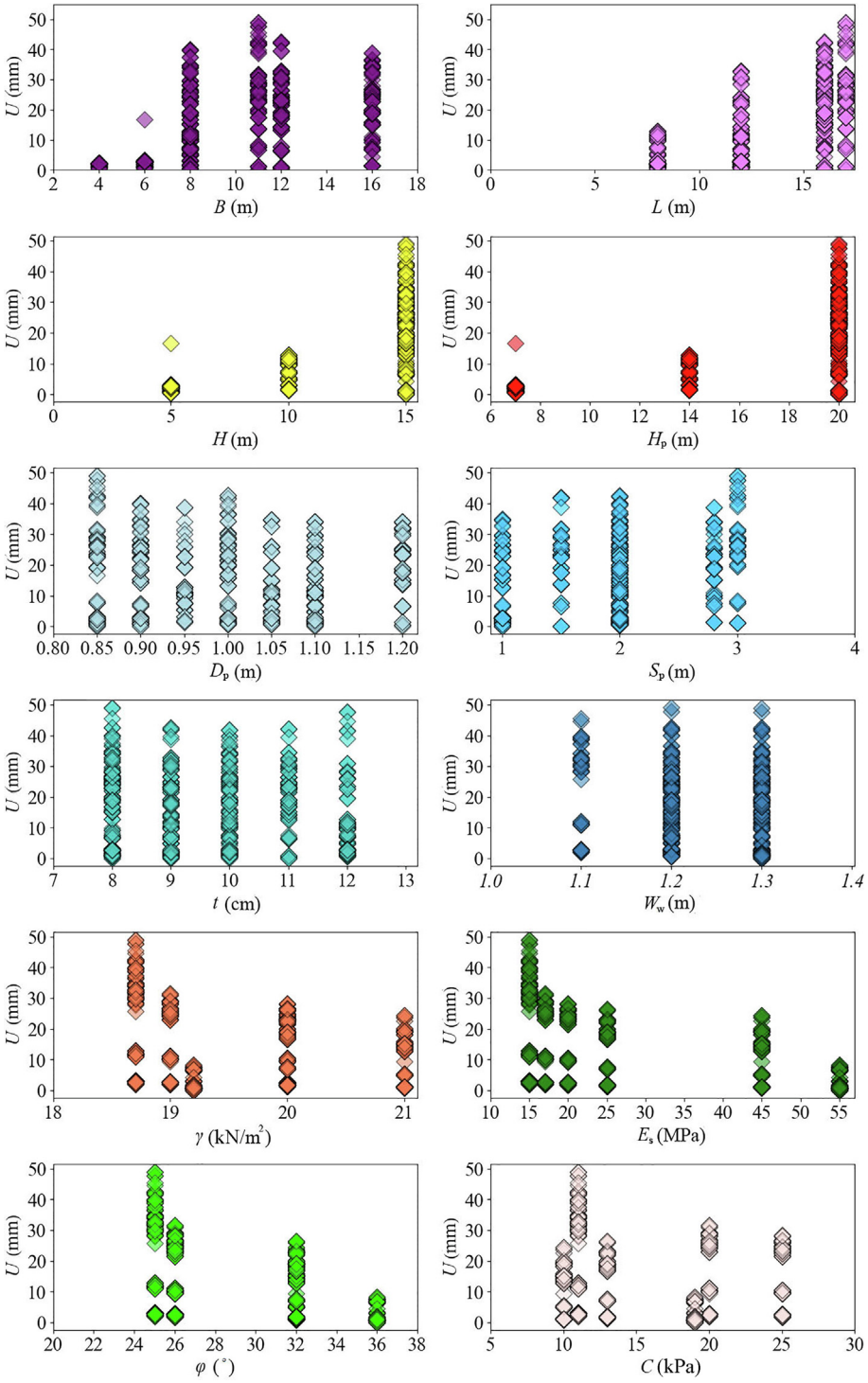

Fig. 3. Scatter plots.

learned weight vector and the bias term in the feature mapping equation.

By integrating the advantages of SVM with the concepts of least squares regression, LS-SVM offers an effective and powerful method for estimating functions. Its applications span various domains, including pattern recognition, regression analysis, and time series prediction.

The LS-SVM model can be mathematically represented as follows:

Minimize:

$$\min_{w,b,e} J(\boldsymbol{w}, e) = \frac{1}{2}\boldsymbol{w}^{\mathrm{T}}\boldsymbol{w} + \frac{1}{2}\gamma\sum_{k=1}^{N} e_k^2; \tag{4}$$

Subject to:

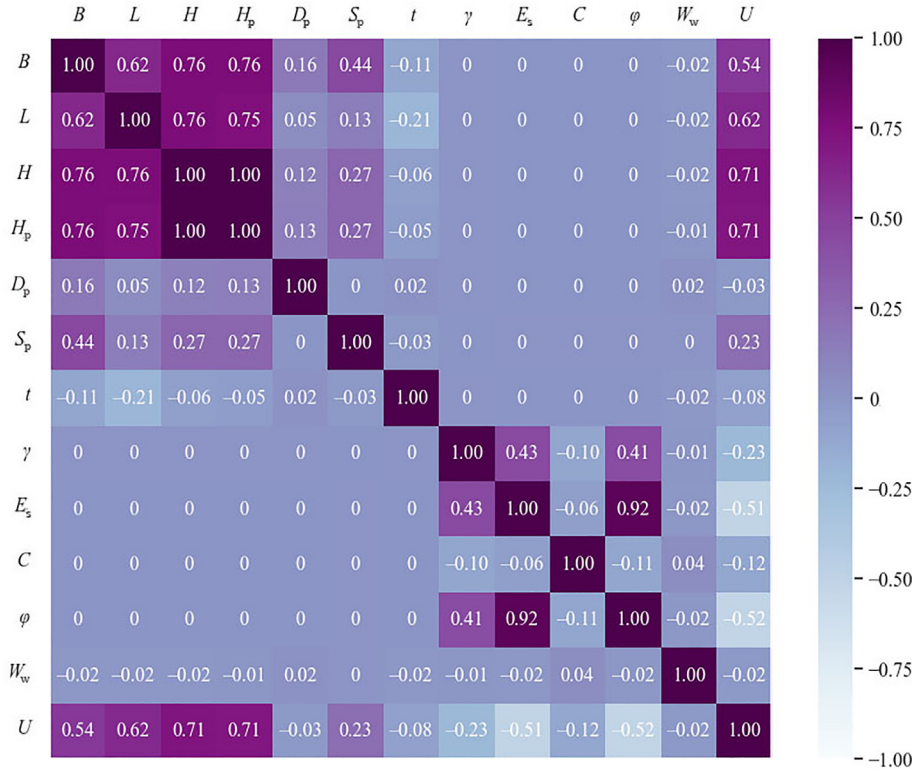

Fig. 4. Correlation heat map is illustrated for the entire dataset.

$$y_k = \boldsymbol{w}^{\mathrm{T}}\varphi(x_k) + b + e_k, k = 1, ..., N, \tag{5}$$

where $\boldsymbol{w}$ is the weight vector; $\varphi(x_k)$ is the feature mapping function; b is the bias term; e_k is the error term for each data point; γ is the regularization parameter that balances the trade-off between model complexity and error minimization; x_k are the slack variables that allow for deviations larger than a specified tolerance.

It is necessary to determine the best regularisation parameter and the error size in the sensitive zone. The sophistication of the prediction is determined by the values chosen for these variables. LS-SVM has limitations that should be considered. It exhibits computational complexity, especially with large datasets and complex feature mappings. The selection of appropriate hyperparameters is critical for optimal performance, and LS-SVM models may lack interpretability compared with other models. Overfitting may occur, especially with complex models or small and noisy datasets. Despite these limitations, LS-SVM remains a valuable tool for function estimation tasks.

4.3 Random forest

Random forest (RF) is a set of tree predictors composed such that the values of each tree depend on the values of a randomly selected vector, which has the same distribution for each tree in the forest. As a bagging ensemble learning technique, RF includes numerous decision trees. This algorithm can be used to perform both regressions and classifications. During training, subsamples are drawn from the full training set by bootstrap sampling, and multiple trees are grown to best fit the data. By averaging the results of numerous trees generated by the training model, the final prediction is produced. The number of trees in the forest (n estimators) and the maximum number of features used in tree development are important factors in RF model (max features) (Breiman, 2001). Although RF is widely used, it can encounter difficulties when dealing with datasets that have a larger number of features as samples. Its performance may also be affected by multicollinearity or dependencies among features. Furthermore, the ensemble nature of Random Forest models limits their interpretability.

In addition, regularisation techniques such as feature bagging and feature subsampling can be applied in RF to avoid overfitting. These techniques help reduce the effect of individual features and increase the diversity among the trees in the forest, improving the generalization performance of the model. By incorporating regularization methods, RF can effectively prevent overfitting and improve the reliability and robustness of the predictions.

4.4 Hyper-parameter tuning

In machine learning, the computer is ideally asked to perform an exploration and automatically select the best model architecture. The parameters that determine the model architecture are called hyperparameters, and the process of defining the best model architecture is called

hyperparameter tuning. Three robust machine learning XGBoost, RF, and LS-SVR models are used to predict the maximum lateral displacement of the pile walls utilizing Optuna. Table 2 shows the tuning factors of the three proposed ML models.

4.5 Error analysis for ML models evaluation

The purpose of developing ML models is to ensure that it is accurate and reliable, can be used in a variety of scenarios, and is as free from bias as possible. Since any modelling method is concerned with accurately representing the truth, error analysis and the resulting actions are crucial. Error analysis can reveal the hotspots and coldspots of the model by identifying, monitoring, and diagnosing the errors in ML predictions. In this study, the mean absolute error (MAE), root mean square error (RMSE), and coefficient of determination (R^2) are three widely used techniques to measure error. An analytical tool used in regression models to determine how much of the observed variation in the dependent variable can be attributed to the independent variable is the coefficient of determination, or R^2. The R^2 value provides information on how well the data fit the regression model according to Eq. (7):

$$R^2 = 1 - \frac{\sum_{i=1}^{m} \left(U_i - U_i^*\right)^2}{\sum_{i=1}^{m} \left(U_i^* - \bar{U}\right)^2}. \tag{7}$$

RMSE quantifies how far a model's predictions deviate from reality. In other words, it assesses how well the observed data match the predictions of the model as reported in Eq. (8):

$$\mathrm{RMSE} = \sqrt{\frac{1}{m} \sum_{i=1}^{m} \left(U_i - U_i^*\right)^2}. \tag{8}$$

MAE measures how far the actual value differs from the predicted value, and values closer to zero show better agreement with the data. It is possible to write the equation as Eq. (9):

$$\mathrm{MAE} = \frac{1}{m} \sum_{i=1}^{m} \left|U_i - U_i^*\right|, \tag{9}$$

where m is the total number of calculated data points; U_i is the predicted values for the wall's maximum displacement; U_i^* is the FEM calculated maximum displacement of the wall values; $\bar{U}$ is the average maximum displacement of the wall.

Table 2
Hyperparameter tuning adopted.

Model	Hyperparameter	Values
RF	max_depth	750
	max_features	–
	*n*_estimators	551
LS-SVR	Kernel Function	RBF
	γ	1000
XGBoost	Booster	gbtree
	Learning rate	0.14
	Max depth	76
	Min child weight	1
	*n*_estimators	100
	reg alpha	0.215
	reg lambda	0.001

5 Results and discussion

5.1 Comparison of the three machine learning methods

The accuracy of the predictions of three intelligent models for the database was measured using statistical and visual analysis. The predictive performance of the three models is compared in Tables 3–5 for a range of training/test split ratios. XGBoost outperforms all models, securing the top spot, followed by LS-SVR and RF, respectively. All three ML models achieved good prediction results when trained ($R^2 > 0.9885$). With R^2 of 0.9991, RMSE of 0.3544, and MAE of 0.1669 in the test phase, XGBoost has been proved to be an effective predictor. The best results were achieved with a training/test split of 70/30.

Figure 5 shows a visual representation of prediction of FEM in function of the maximum displacement for three ML methods. From these plots, it is clear that the distribu-

Table 3
The statistical parameters computed to evaluate the efficiency of the established models (80/20).

Model	Training dataset			Testing dataset		
	R^2	RMSE	MAE	R^2	RMSE	MAE
XGBoost	0.9999	0.0909	0.0569	0.9991	0.3923	0.1817
RF	0.9972	0.6402	0.2525	0.9937	0.9662	0.4866
LS-SVR	0.9940	0.9400	0.4617	0.9929	0.9950	0.4865

Table 4
The statistical parameters computed to evaluate the efficiency of the established models (75/25).

Model	Training dataset			Testing dataset		
	R^2	RMSE	MAE	R^2	RMSE	MAE
XGBoost	0.9995	0.2605	0.1348	0.9980	0.5394	0.2856
RF	0.9970	0.6668	0.2667	0.9930	1.0105	0.5170
LS-SVR	0.9946	0.8940	0.4511	0.9913	1.1050	0.5133

Table 5
The statistical parameters computed to evaluate the efficiency of the established models (70/30).

Model	Training dataset			Testing dataset		
	R^2	RMSE	MAE	R^2	RMSE	MAE
XGBoost	0.9999	0.0637	0.0428	0.9991	0.3544	0.1669
RF	0.9972	0.6443	0.2567	0.9924	1.0480	0.5675
LS-SVR	0.9976	0.6060	0.2298	0.9964	0.7060	0.2475

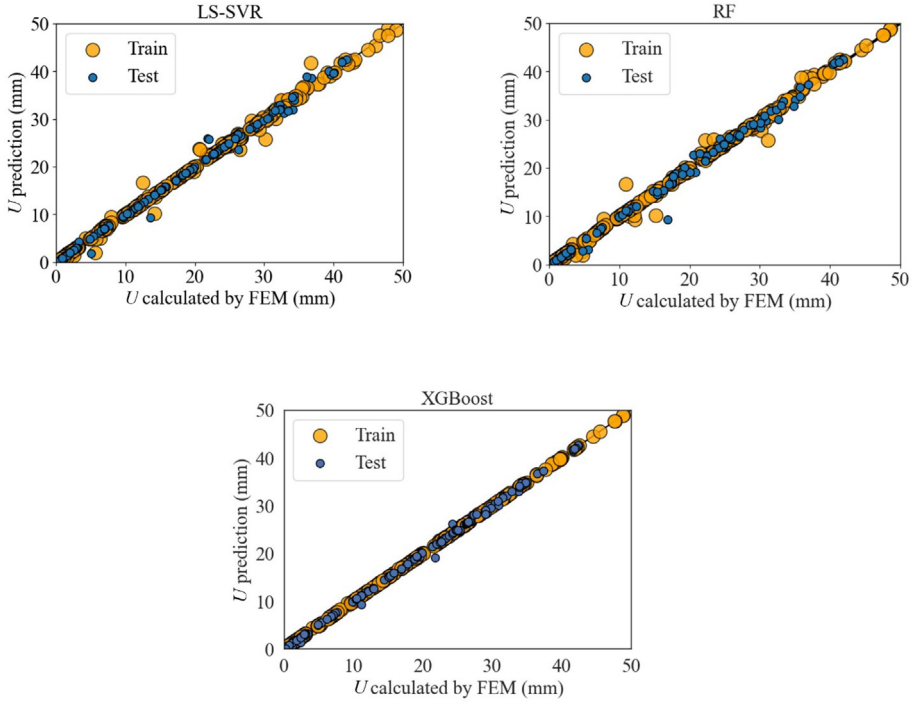

Fig. 5. Predictions of the three ML models for maximum displacement are compared with the calculations of FEM using the cross plots.

tion of the predicted maximum displacement of the training and testing data closely matches estimated FEM maximum displacement (slope = 1). The R^2 value of 99.91% shows that the FEM result and the prediction agree very well. The XGBoost method can be used to predict the maximum displacement of soldier pile walls.

Figure 6 shows a bar chart comparing the R^2, RMSE and MAE indicators for the three proposed ML models evaluated against the entire database. In Fig. 6, it can be seen that the XGBoost model has the highest performance on the training and testing data, which is the most interesting part of this graph. Figure 6 shows that the statistical performance of RF was the weakest in the training and testing phase. MAE error performance of LS-SVR is comparable to that of XGBoost. Instead of reading raw reports, it is always better to present a visual representation of the collected data to identify trends and unique experiences. Figures 7 and 8 show a visual representation of the raw data from this perspective. A Taylor chart represents the comparison of multiple models with a baseline. The diagram shows how two values (the "predicted model" and the "reference" values) are statistically related. Three different statistical metrics (correlation, SD, and centred RMSE) are displayed in the two-dimensional space of the graph. The values of the ideal model are closer to or identical with the reference point.

The Regression Error Characteristic (REC) curve, originally proposed by Bi and Bennett (2003), is a graphical representation for evaluating the performance of regression models. It is similar to the Receiver Operating Characteristic curve used in classification tasks, but is specifically tailored to regression analysis. The curve represents the

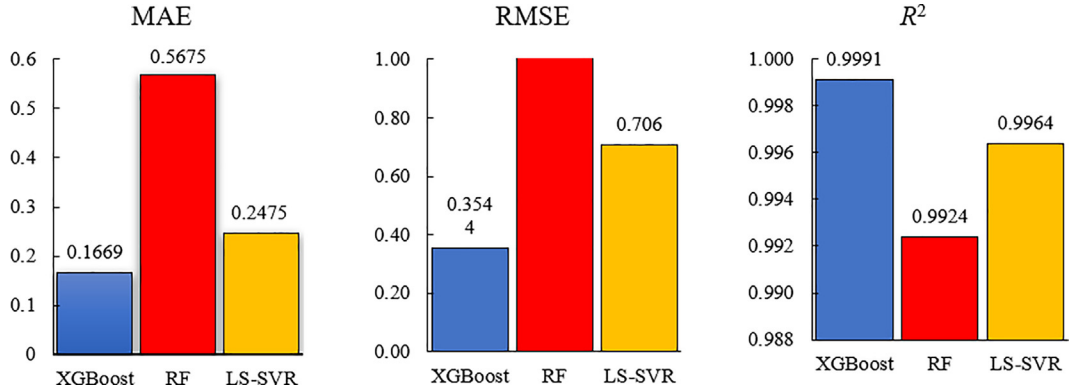

Fig. 6. Statistical measures of the three ML models.

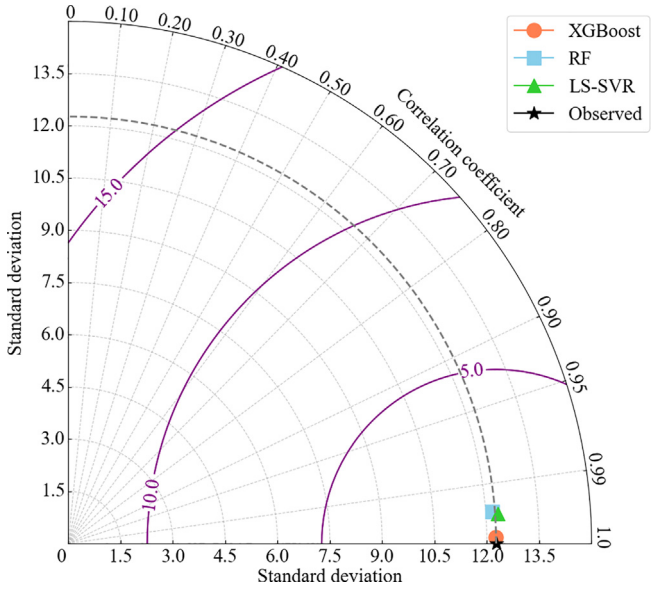

Fig. 7. Taylor diagram representation for the predictive performance (train dataset).

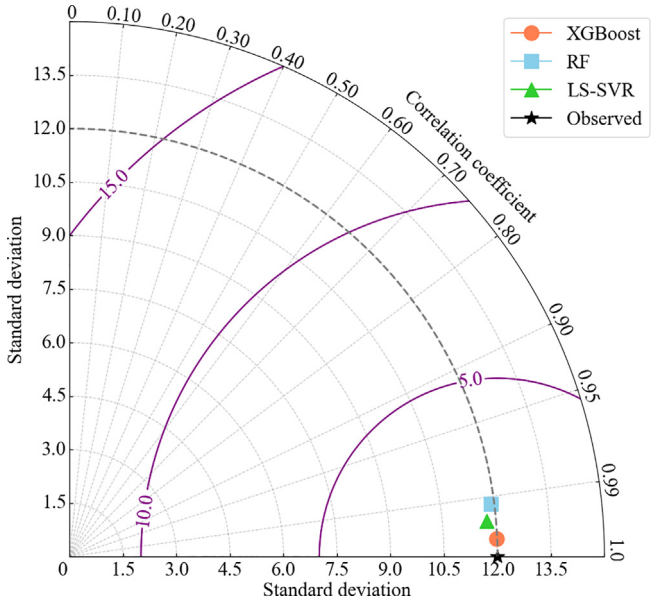

Fig. 8. Taylor diagram representation for the predictive performance (test dataset).

accuracy of a regression model as a function of the deviation threshold. The deviation threshold represents the acceptable degree of difference between the predicted and the actual values of the target variable. By varying the deviation threshold, the REC curve shows how the accuracy of the model changes over different levels of prediction tolerance.

Area Under the Curve (AUC) is a metric calculated based on the REC curve. It quantifies the overall accuracy of the regression model. An AUC of 1 indicates perfect prediction, while an AUC of 0.5 indicates random guessing. The REC curve and AUC provide valuable insights into the predictive ability and accuracy of regression models.

The AUC results of the training and test datasets show the performance of the three regression models (Fig. 9): XGBoost, LS-SVR, and RF. Of these models, XGBoost achieved the highest AUC of 0.980 for the training dataset, indicating its strong predictive ability. For the test dataset, both XGBoost and LS-SVR exhibited good generalisation ability with AUC values of 0.961 and 0.959, respectively. Although RF had a slightly lower AUC value of 0.948 on the test data set, it still showed a reasonable level of performance. Overall, XGBoost, LS-SVR and, RF are promising for the given task, with XGBoost performing

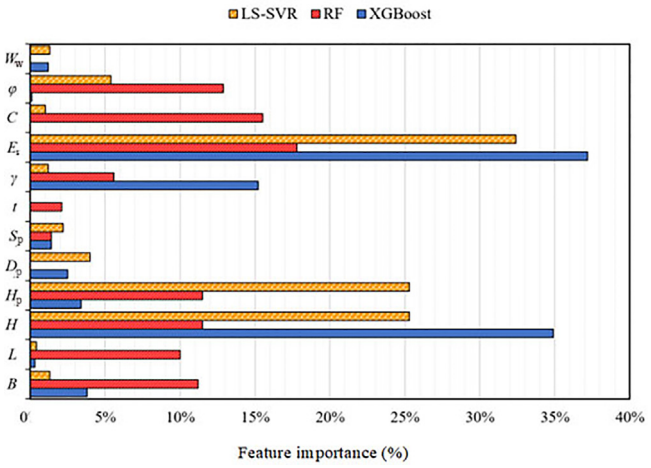

Fig. 10. Feature importance diagram signifies the inputs impact on the maximum lateral wall displacement in soldier pile walls.

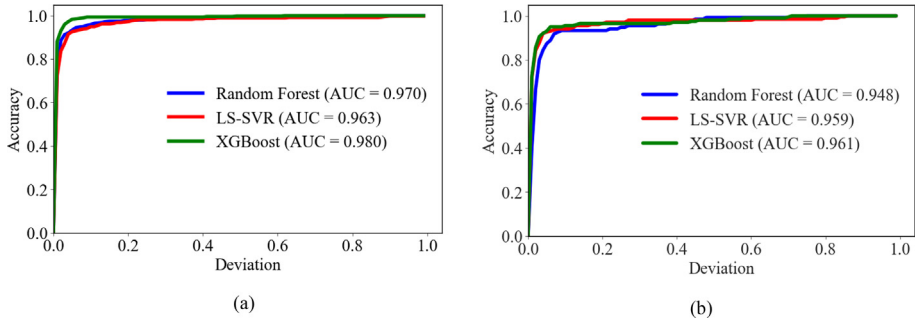

Fig. 9. Comparison between the REC curves for (a) train, and (b) test.

Table 6
Feature importance on maximum soldier pile wall displacement.

Model	B	L	H	H_p	D_p	S_p	t	γ	E_s	C	φ	W_w
XGBoost	3.8%	0.3%	34.9%	3.4%	2.5%	1.4%	0.0%	15.2%	37.2%	0.0%	0.1%	*1.2%*
LS-SVR	11.2%	10.0%	11.5%	11.5%	0.0%	1.4%	2.1%	5.6%	17.8%	15.5%	12.9%	0.0%
RF	1.3%	0.4%	25.3%	25.3%	4.0%	2.2%	0.0%	1.2%	32.4%	1.0%	5.4%	1.3%

exceptionally well and both LS-SVR and RF offering competitive performance on unseen data.

5.2 Input feature importance analysis

As it can be seen in Fig. 10 and Table 6, the feature importance shows that soil elastic modulus and excavation height are the most influential input variables, followed by soil unit weight and pile height with feature importance of 37.2%, 34.2%, 15.2%, and 3.8% for XGBoost, respectively. Further observation implies that in addition to the soil elastic modulus, excavation height, and pile height, cohesion, and soil friction angle are very important in determining the maximum displacement of the soldier pile wall for LS-SVR with feature significance of 17.8%, 11.5%, 11.5%, 15.5%, and 12.9% respectively. Almost similar results are obtained with the RF method. Although the soil elastic modulus, the excavation height, and pile height play the most important role, with a feature importance of 32.4%, 25.3%, and 25.3%, the friction angle is very important with a value of 5.4% for RF.

6 Conclusions

In this paper, the maximum displacement of soldier pile walls was predicted using a database of 675 FEM calculated data points and three robust intelligent models (XGBoost, RF and LS-SVR). Statistical indicators and visual analysis were used to analyse the accuracy and stability of the three intelligent models. As an added bonus, a sensitivity analysis was performed to find out the most important factor of the optimal intelligent model. The main conclusions of the study are as follows:

(1) To save time and economic resources, this study has shown a way to implement intelligent algorithms for predicting the maximum displacement of soldier pile wall due to excavation.
(2) The maximum displacement of the soldier pile wall can be best estimated by the XGBoost model. The XGBoost outperformed the LS-SVR and RF models in all evaluation metrics. It achieved the lowest MAE and RMSE, indicating lower prediction errors compared with RF and LS-SVR. In addition, XGBoost had a nearly perfect R^2 results.
(3) The significant of the feature importance for XGBoost is defined as follows: modulus of elasticity of soil > excavation height > soil unit weight > pile height. While for RF it is modulus of elasticity of soil > excavation height > pile height > soil friction angle > excavation length (B).
(4) This result shows that the width of the excavation (L) parallel to the deformation and the thickness of the shotcrete has no influence on the maximum lateral displacement of the soldier pile walls when XGBoost and RF are used.
(5) The advantage of this study is that it is a promising way to reduce time and labour costs, while providing a smart method to predict the maximum lateral displacement of soldier pile walls.

However, the proposed intelligent methods have the following limitations:

(1) The developed intelligent models are used to predict the maximum lateral displacement of soldier pile walls only in similar statistical characterisation.
(2) Although the LS-SVR and RF models are less accurate than the XGBoost model, they still provide good prediction results for the maximum lateral displacement of soldier pile walls for numerical models.

Declaration of competing interest

The authors declare that they have no known competing financial interests or personal relationships that could have appeared to influence the work reported in this paper.

Acknowledgment

This work was not supported by any funding source.

References

Addenbrooke, T. I., Potts, D. M., & Dabee, B. (2000). Displacement flexibility number for multipropped retaining wall design. *Journal of Geotechnical and Geoenvironmental Engineering, 126*(8), 718–726.
Akan, R. (2022). Estimation of the maximum bending moment of cantilever sheet pile walls by using multiple linear regression analysis. *Mühendislik Bilimleri ve Tasarım Dergisi, 10*(1), 247–256.
Akiba, T., Sano, S., Yanase, T., Ohta, T., & Koyama, M. (2019). Optuna: A next-generation hyperparameter optimization framework. In *Proceedings of the 25th ACM SIGKDD International Conference on Knowledge Discovery & Data Mining* (pp. 2623–2631).
Alkroosh, I., & Nikraz, H. (2012). Predicting axial capacity of driven piles in cohesive soils using intelligent computing. *Engineering Applications of Artificial Intelligence, 25*(3), 618–627.
Athmarajah, G., & De Silva, L. I. N. (2019). Analysis of stability enhancement of soldier pile retaining wall. *Moratuwa Engineering Research Conference (MERCon), 2019*, 644–650.

Bekdaş, G., Arama, Z. A., Kayabekir, A. E., & Geem, Z. W. (2020). Optimal design of cantilever soldier pile retaining walls embedded in frictional doils with harmony search algorithm. *Applied Sciences, 10*(9), 3232.

Bi, J., & Bennett, K. P. (2003). Regression error characteristic curves. In *Proceedings of the 20th International Conference on Machine Learning (ICML-03)*, 43–50.

Bica, A. V. D., & Clayton, C. R. I. (1998). An experimental study of the behaviour of embedded lengths of cantilever walls. *Géotechnique, 48*(6) , 731–745.

Breiman, L. (2001). Random forests. *Machine Learning, 45*(1), 5–32.

Buslov, A., & Margolin, V. (2018). The influence of the second row of piles in double-row pile retaining walls with the stabilization of landslide. *IOP Conference Series: Materials Science and Engineering, 365*, 052006.

Ceryan, N., Okkan, U., Samui, P., & Ceryan, S. (2013). Modeling of tensile strength of rocks materials based on support vector machines approaches: Modeling of tensile strength based on svm approaches. *International Journal for Numerical and Analytical Methods in Geomechanics, 37*(16), 2655–2670.

Chalmovsky, J., Fiala, R., & Mica, L. (2011). Soldier pile walls–3D numerical analysis of soldier pile embedment. *COMPLAS XI: Proceedings of the XI International Conference on Computational Plasticity: Fundamentals and Applications*, 1274–1283.

Chavda, J. T., Solanki, C. H., & Desai, A. K. (2019). Lateral response of contiguous pile wall subjected to staged excavation: Physical and numerical investigations. *Indian Geotechnical Journal, 49*(1), 90–99.

Chen, T., & Guestrin, C. (2016). Xgboost: A scalable tree boosting system. In *Proceedings of the 22nd Acm Sigkdd International Conference on Knowledge Discovery and Data Mining* (pp. 785–794).

Cheuk, C. Y., Ng, C. W. W., & Sun, H. W. (2005). Numerical experiments of soil nails in loose fill slopes subjected to rainfall infiltration effects. *Computers and Geotechnics, 32*(4), 290–303.

Dong, Y., Burd, H., Houlsby, G., & Hou, Y. (2014). Advanced finite element analysis of a complex deep excavation case history in Shanghai. *Frontiers of Structural and Civil Engineering, 8*(1), 93–100.

Elbaz, K., Shen, S.-L., Tan, Y., & Cheng, W.-C. (2018). Investigation into performance of deep excavation in sand covered karst: A case report. *Soils and Foundations, 58*(4), 1042–1058.

Gajan, S. (2011). Normalized relationships for depth of embedment of sheet pile walls and soldier pile walls in cohesionless soils. *Soils and Foundations, 51*(3), 559–564.

Goh, A. T. C., Zhang, F., Zhang, W., Zhang, Y., & Liu, H. (2017). A simple estimation model for 3D braced excavation wall deflection. *Computers and Geotechnics, 83*, 106–113.

Gopal Madabhushi, S. P., & Chandrasekaran, V. S. (2005). Rotation of cantilever sheet pile walls. *Journal of Geotechnical and Geoenvironmental Engineering, 131*(2), 202–212.

Hashash, Y. M. A., & Whittle, A. J. (1996). Ground movement prediction for deep excavations in soft clay. *Journal of Geotechnical Engineering, 122*(6), 474–486.

Hong, S. H., Lee, F. H., & Yong, K. Y. (2003). Three-dimensional pile-soil interaction in soldier-piled excavations. *Computers and Geotechnics, 30*(1), 81–107.

Hsiung, B.-C.-B. (2009). A case study on the behaviour of a deep excavation in sand. *Computers and Geotechnics, 36*(4), 665–675.

Hsiung, B.-C.-B., Yang, K.-H., Aila, W., & Hung, C. (2016). Three-dimensional effects of a deep excavation on wall deflections in loose to medium dense sands. *Computers and Geotechnics, 80*, 138–151.

Hu, Y., Lin, P., Guo, C., & Mei, G. (2020). Assessment and calibration of two models for estimation of soil nail loads and system reliability analysis of soil nails against internal failures. *Acta Geotechnica, 15*(10), 2941–2968.

Huang, Z., Zhang, D., & Zhang, D. (2021). Application of ANN in predicting the cantilever wall deflection in undrained clay. *Applied Sciences, 11*(20), 9760.

Huang, Z.-K., Zhang, D.-M., & Xie, X.-C. (2022). A practical ANN model for predicting the excavation-induced tunnel horizontal displacement in soft soils. *Underground Space, 7*(2), 278–293.

Ismail, A., & Jeng, D.-S. (2011). Modelling load–settlement behaviour of piles using high-order neural network (HON-PILE model). *Engineering Applications of Artificial Intelligence, 24*(5), 813–821.

Jan, J. C., Hung, S.-L., Chi, S. Y., & Chern, J. C. (2002). Neural network forecast model in deep excavation. *Journal of Computing in Civil Engineering, 16*(1), 59–65.

Kunasegaram, V., & Takemura, J. (2021). Deflection and failure of high-stiffness cantilever retaining wall embedded in soft rock. *International Journal of Physical Modelling in Geotechnics, 21*(3), 114–134.

Kung, G. T. C., Hsiao, E. C. L., Schuster, M., & Juang, C. H. (2007). A neural network approach to estimating deflection of diaphragm walls caused by excavation in clays. *Computers and Geotechnics, 34*(5), 385–396.

Lee, C.-J., Wei, Y.-C., Chen, H.-T., Chang, Y.-Y., Lin, Y.-C., & Huang, W.-S. (2011). Stability analysis of cantilever double soldier-piled walls in sandy soil. *Journal of the Chinese Institute of Engineers, 34*(4), 449–465.

Liu, L., Wu, R., Congress, S. S. C., Du, Q., Cai, G., & Li, Z. (2021). Design optimization of the soil nail wall-retaining pile-anchor cable supporting system in a large-scale deep foundation pit. *Acta Geotechnica, 16*(7), 2251–2274.

Moormann, C. (2004). Analysis of wall and ground movements due to deep excavations in soft soil based on a new worldwide database. *Soils and Foundations, 44*(1), 87–98.

Ou, X., Zhang, X., Fu, J., Zhang, C., Zhou, X., & Feng, H. (2020). Cause investigation of large deformation of a deep excavation support system subjected to unsymmetrical surface loading. *Engineering Failure Analysis, 107*, 104202.

Perko, H. A., & Boulden, J. J. (2008). Lateral earth pressure on lagging in soldier pile wall systems. *DFI Journal - The Journal of the Deep Foundations Institute, 2*(1), 52–60.

Pradeep, T., GuhaRay, A., Bardhan, A., Samui, P., Kumar, S., & Armaghani, D. J. (2022). Reliability and prediction of embedment depth of sheet pile walls using hybrid ANN with optimization techniques. *Arabian Journal for Science and Engineering*.

Ramadan, M. I., & Meguid, M. (2020). Behavior of cantilever secant pile wall supporting excavation in sandy soil considering pile-pile interaction. *Arabian Journal of Geosciences, 13*(12), 466.

Ramadan, M. I., Ramadan, E. H., & Khashila, M. M. (2018). Cantilever contiguous pile wall for Ssupporting excavation in clay. *Geotechnical and Geological Engineering, 36*(3), 1545–1558.

Rashidi, F., & Shahir, H. (2019). Numerical investigation of anchored soldier pile wall performance in the presence of surcharge. *International Journal of Geotechnical Engineering, 13*(2), 162–171.

Razeghi, H. R., Nakhaee, M., & Ghareh, S. (2021). Effect of geometrical properties on mechanical behavior of cantilever pile walls (CPW): Centrifuge tests. *International Journal of Civil Engineering, 19*(11), 1251–1267.

Samui, P. (2011). Prediction of pile bearing capacity using support vector machine. *International Journal of Geotechnical Engineering, 5*(1), 95–102.

Samui, P. (2013). Support vector classifier analysis of slope. *Geomatics, Natural Hazards and Risk, 4*(1), 1–12.

Samui, P., Kim, D., & Sitharam, T. G. (2011). Support vector machine for evaluating seismic-liquefaction potential using shear wave velocity. *Journal of Applied Geophysics, 73*(1), 8–15.

Singh, V. P., & Sivakumar Babu, G. L. (2010). 2D Numerical simulations of soil nail walls. *Geotechnical and Geological Engineering, 28*(4), 299–309.

Su, J., Wang, Y., Niu, X., Sha, S., & Yu, J. (2022). Prediction of ground surface settlement by shield tunneling using XGBoost and Bayesian Optimization. *Engineering Applications of Artificial Intelligence, 114*, 105020.

Suykens, J. A. K., De Brabanter, J., Lukas, L., & Vandewalle, J. (2002). Weighted least squares support vector machines: Robustness and sparse approximation. *Neurocomputing, 48*(1–4), 85–105.

Tan, Y., & Wei, B. (2012). Observed behaviors of a long and deep excavation constructed by cut-and-cover technique in Shanghai soft clay. *Journal of Geotechnical and Geoenvironmental Engineering, 138*(1), 69–88.

Vermeer, P. A., Punlor, A., & Ruse, N. (2001). Arching effects behind a soldier pile wall. *Computers and Geotechnics, 28*(6–7), 379–396.

Wong, K. S., & Broms, B. B. (1989). Lateral wall deflections of braced excavations in clay. *Journal of Geotechnical Engineering, 115*(6), 853–870.

Ye, J., & He, X. (2022). Evaluation of flexural stiffness on mechanical property of dual row retaining pile wall. *Mechanics of Advanced Materials and Structures, 29*(7), 963–974.

Yodsomjai, W., Lai, V. Q., Banyong, R., Chauhan, V. B., Thongchom, C., & Keawsawasvong, S. (2022). A machine learning regression

approach for predicting basal heave stability of braced excavation in non-homogeneous clay. *Arabian Journal of Geosciences, 15*(9), 873.
Yuan, J., Lin, P., Huang, R., & Que, Y. (2019). Statistical evaluation and calibration of two methods for predicting nail loads of soil nail walls in China. *Computers and Geotechnics, 108*, 269–279.
Zhang, D., Shen, Y., Huang, Z., & Xie, X. (2022). Auto machine learning-based modelling and prediction of excavation-induced tunnel displacement. *Journal of Rock Mechanics and Geotechnical Engineering*, S1674775522000786.
Zhang, L., Zhou, J., Zhou, S., & Xu, Z. (2022). Numerical spring-based trapdoor test on soil arching in pile-supported embankment. *Computers and Geotechnics, 148*, 104765.
Zhang, R., Wu, C., Goh, A. T. C., Böhlke, T., & Zhang, W. (2021). Estimation of diaphragm wall deflections for deep braced excavation in anisotropic clays using ensemble learning. *Geoscience Frontiers, 12*(1), 365–373.
Zhang, W., Zhang, R., Wu, C., Goh, A. T. C., Lacasse, S., Liu, Z., & Liu, H. (2020). State-of-the-art review of soft computing applications in underground excavations. *Geoscience Frontiers, 11*(4), 1095–1106.
Zhao, H., Liu, W., Shi, P., Du, J., & Chen, X. (2021). Spatiotemporal deep learning approach on estimation of diaphragm wall deformation induced by excavation. *Acta Geotechnica, 16*(11), 3631–3645.